
Range-aware Positional Encoding via High-order Pretraining: Theory and Practice

Viet Anh Nguyen
FPT Software AI Center
anhnv117@fpt.com

Nhat Khang Ngo
Mila - Quebec AI Institute, McGill University
khang.ngo@mila.quebec

Truong Son Hy*
University of Alabama at Birmingham
thy@uab.edu

Abstract

Unsupervised pre-training on vast amounts of graph data is critical in real-world applications wherein labeled data is limited, such as molecule properties prediction or materials science. Existing approaches pre-train models for specific graph domains, neglecting the inherent connections within networks. This limits their ability to transfer knowledge to various supervised tasks. In this work, we propose a novel pre-training strategy on graphs that focuses on modeling their multi-resolution structural information, allowing us to capture global information of the whole graph while preserving local structures around its nodes. We extend the work of **Wavelet Positional Encoding** (WavePE) from Ngo et al. [1] by pre-training a **High-Order Permutation-Equivariant Autoencoder** (HOPE-WavePE) to reconstruct node connectivities from their multi-resolution wavelet signals. Unlike existing positional encodings, our method is designed to become sensitivity to the input graph size in downstream tasks, which efficiently capture global structure on graphs. Since our approach relies solely on the graph structure, it is also domain-agnostic and adaptable to datasets from various domains, therefore paving the way for developing general graph structure encoders and graph foundation models. We theoretically demonstrate that there exists a parametrization of such architecture that it can predict the output adjacency up to arbitrarily low error. We also evaluate HOPE-WavePE on graph-level prediction tasks of different areas and show its superiority compared to other methods.

1 Introduction

One of the fastest-growing areas in machine learning is graph representation learning, with impactful applications in biomedicine, molecular chemistry, and network science. Most graph neural networks (GNNs) rely on the message-passing framework that processes graph-structured data by exchanging the vectorized information between nodes on graphs along their edges. Albeit achieving remarkable results in a wide range of tasks on graph data, message-passing neural networks (MPNNs) possess several fundamental limits, including expressiveness [2–6], over-smoothing [7], and over-squashing [8]. In recent years, transformer-based architectures [1, 9–12] have emerged as powerful alternatives to address the mentioned issues of MPNN. The self-attention mechanism in conventional transformers computes the pairwise interactions between the input tokens, enabling the modeling of long-range interactions between distant tokens and overcoming information bottlenecks on graphs [13–15]. While applying transformers to graphs offers advantages, it often necessitates a trade-off between computational resources and performance, particularly when scaling models to massive datasets with thousands to millions of nodes, like citation networks. Augmenting virtual nodes (VN) to the original

*Corresponding Author

graph’s nodes, which allows global connections among these nodes, has emerged as a promising strategy to balance these two objectives [13, 15–17].

However, graph transformers (GTs) and VN-augmented MPNNs disregard the underlying structure of graph data by altering inherent connections among the nodes (i.e., shortening all paths to two). This disregard may explain their limitations in several graph-level prediction tasks. To address this, positional and structural encodings (PSE) are commonly used to enhance structural information in modern GNNs. However, existing PSE encoding methods often have limitations in terms of task specificity. For instance, random walk encodings [18, 19] excel with small molecules, while Laplacian encoding [11] captures long-range interactions effectively. Meanwhile, Ngo et al. [1] propose Wavelet positional encoding (WavePE), a PSE encoding technique that models the node interactions at multiple scales. By leveraging multi-resolution analysis based on Wavelet Transform on graphs [20–24], WavePE enables neural networks to capture a comprehensive range of structural information, from local to global properties.

Real-world applications of learning methods on graphs face two challenges [25, 26]. First, in fields like biology and chemistry, task-specific labeled data is scarce, and acquiring them requires significant time and resources [27]. Second, real-world graph datasets often contain out-of-distribution samples; for example, newly synthesized molecules may have different structures from those in the training set, leading to inaccurate prediction of supervised learning models. Meanwhile, transfer learning is a promising approach to overcoming these challenges. Our key insight is that graph data possesses two distinct feature types: (1) domain-specific (e.g., atom types in molecules or user names citation networks) and (2) topological features. While the former depends on specific domains, the latter is a general form of graph data. This observation gives rise to our idea of *structural pretraining*, wherein we pretrain a model on topological features of graph data. Specifically, given the Wavelet signals of a graph, we train an autoencoder to reconstruct its adjacency matrix. The graph wavelet signals are defined based on functions of eigenvalues of the graph Laplacian at *multiple resolutions*, representing general forms of connectivities among nodes on the graphs [1, 23, 24]. As a result, a model trained on these features should be able to capture the underlying patterns of different graph structures and generalize well to downstream tasks. After pretraining, we can use this pretrained model as a general structural encoder that extracts node structural features, which are passed to graph neural networks along with domain-specific features for predicting task-specific properties.

1.1 Contribution

In this work, we propose a new pretraining approach on graphs that leverages the reconstruction of graph structures from the Wavelet signals to generalize structural information on graph data, thus enabling transfer learning to various downstream tasks across various domains of different ranges. Our contributions are three-fold as follows:

- We propose a high-order structural pretrained models for graph-structured data and a loss-masking technique that leverages high-order interactions of nodes on graphs while being aware of the graph size and diameter, therefore capturing better positional and structural information.
- We theoretically prove that pretraining by reconstruction with multi-resolution Wavelet signals can make autoencoder learn node state after an arbitrarily walk of length d , which can contain both local and global information of graph structures. We also analyzed the width required for the latent space of the autoencoder to ensure such performance and also propose a low-rank alternative.
- We empirically show that such pretraining scheme can enhance the performance of supervised models when fine-tuned on downstream datasets of different domains, indicating the generalizability and effectiveness of pretrained structural encoding compared with other domain-specific pretraining methods.

2 Related work

Graph Positional and Structural Encodings. Node positional encodings are augmented into node features to preserve the graph structure information and increase the expressiveness of MPNNs [18, 28–30] and Graph Transformers [9, 19, 31–34]. Many recent works directly use the graph

Laplacian eigenvectors as node positional encodings and combine them with domain-specific node features [9, 31, 33, 34]. Other works use several approaches to encode graph’s structural information, including random walks [18, 19, 35, 36], diffusion kernels on graphs [1, 10, 35], shortest paths [36, 37], and unsupervised node embedding methods [29, 38]. Our work builds on similar approaches to Wang et al. [29] and Liu et al. [38], where we pre-train an encoder to capture node positional information in an unsupervised setting. However, these pretraining methods either struggle to capture long-range information, lack equivariant constraints that is intrinsic on graphs, or being domain-specific on certain datas and fail in terms of transferrability. We overcome both of these shortcomings by designing a permutation equivariant autoencoder that only focus on the intrinsic structure of the graph, neglecting domain-specific features while being able to learn long hops neighbor in a graph. These learned positional features can be adapted to various downstream tasks and generalize well to domain-specific datasets. Furthermore, we theoretically demonstrate that our method is general and can express several common positional encoding schemes.

Pretraining on Graphs. In the age of modern deep learning, pre-training models on massive unlabeled datasets and then fine-tuning them on smaller, labeled datasets has proven remarkably successful in areas like natural language processing [39, 40] and computer vision [41, 42]. For graph-structured data, self-supervised pre-training is a growing area of research, with contrastive learning being a popular approach [43–47]. While these methods can enhance performance on various downstream tasks, their reliance on domain-specific features to create different views of the input graphs limits their transferability to other domains. For instance, models pretrained on small molecules struggle to adapt to other graph types like citation networks, proteins, or code repositories. Our work aims to propose a more generalizable graph pre-training method that relies only on graph *intrinsic features*, i.e. adjacency matrices, which can be trained on unfeatured data and easily transferred for predicting properties of small graph datasets in arbitrary domains. To solidify such transferrability, we elevate a pretraining method that learn a spectrum of range on graphs. This way, structures on different domains belonging to the spectrum can still be captured without being reliant on domain features.

3 Notations and Preliminaries

3.1 Notations

In this work, we define a graph $G = (V, E, \mathbf{A})$, where V and E denote node and edge sets, respectively, and $\mathbf{A} \in \mathbb{R}^{n \times n}$ is the adjacency matrix. The normalized graph Laplacian is computed as: $\tilde{L} = \mathbf{I}_n - \mathbf{D}^{-1/2} \mathbf{A} \mathbf{D}^{-1/2}$ where \mathbf{D} is the diagonal degree matrix, and \mathbf{I}_n is the identity matrix.

3.2 Permutation equivariant function

In this section, we formally define permutation symmetry, i.e. symmetry to the action of the symmetric group, \mathbb{S}_n , and construct permutation-equivariant neural networks to encode graph wavelets. An element $\sigma \in \mathbb{S}_n$ is a permutation of order n , or a bijective map from $\{1, 2, \dots, n\}$ to $\{1, 2, \dots, n\}$. We present each element σ in \mathbb{S}_n as a permutation matrix $\mathbf{P}_\sigma \in \mathbb{R}^{n \times n}$. For example, the action of \mathbb{S}_n on an adjacency matrix $\mathbf{A} \in \mathbb{R}^{n \times n}$ and on a latent matrix (i.e. node embedding matrix) $\mathbf{Z} \in \mathbb{R}^{n \times d_z}$ are:

$$\sigma(\mathbf{A}) = \mathbf{P}_\sigma \mathbf{A} \mathbf{P}_\sigma^\top, \quad \sigma(\mathbf{Z}) = \mathbf{P}_\sigma \mathbf{Z},$$

for $\sigma \in \mathbb{S}_n$. Here, the adjacency matrix \mathbf{A} is a second-order tensor with a single feature channel, while the latent matrix \mathbf{Z} is a first-order tensor with d_z feature channels. Likewise, the permutation on a k -th order tensor $\mathbf{X} \in \mathbb{R}^{n^k \times d}$ operate on the first k dimensions of \mathbf{X} .

Furthermore, we define permutation equivariance on non-homogeneous order functions.

Definition 1. A \mathbb{S}_n -equivariant (or permutation equivariant) function is a function $f: \mathbb{R}^{n^k \times d} \rightarrow \mathbb{R}^{n^{k'} \times d'}$ that satisfies $f(\sigma(\mathbf{X})) = \sigma(f(\mathbf{X}))$ for all $\sigma \in \mathbb{S}_n$ and $\mathbf{X} \in \mathbb{R}^{n^k \times d}$.

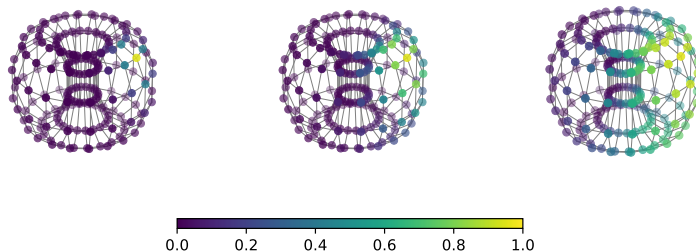


Figure 1: Visualization of graph Wavelet on the geometric graph of a torus. The low scaling factor s results in a highly localized structure around the center node (yellow), while higher factors can lead to smoother signals that can spread out to a larger part of the graph with scaling factor 4, 15 and 50 respectively.

4 Methodology

4.1 Spectral Graph Wavelet Tensors

As the normalized graph Laplacian $\tilde{L} \in \mathbb{R}^{n \times n}$ is symmetric when G is undirected, we can decompose it into a complete set of orthonormal eigenvectors $U = (u_1, u_2, \dots, u_n)$ wherein u_i is associated with a real and non-negative eigenvalue λ_i as:

$$\tilde{L} = U\Lambda U^T, \quad (1)$$

where $\Lambda = \text{diag}(\lambda_1, \dots, \lambda_n)$ is the diagonal matrix of eigenvalues. The graph Wavelet transforms construct a set of spectral graph Wavelet as bases to project the graph signal from the vertex domain to the spectral domain as:

$$\psi_s = U\Lambda_s U^T, \quad (2)$$

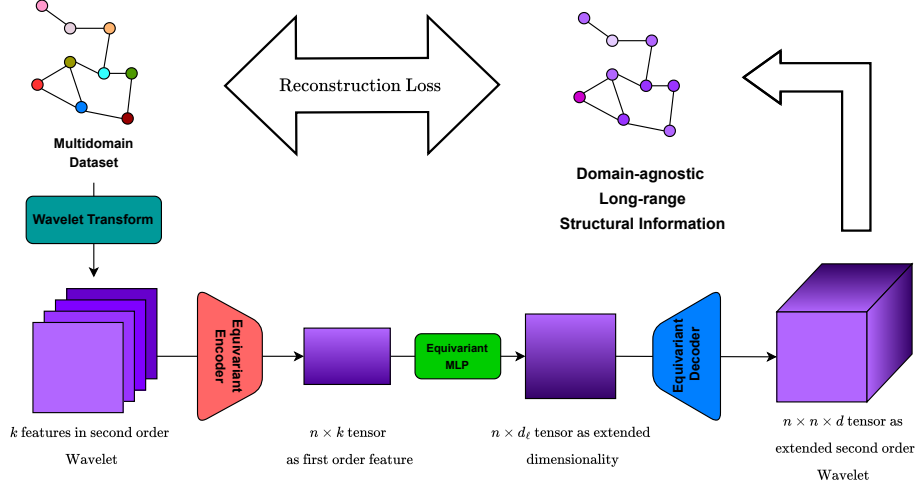
here, $\Lambda_s = \text{diag}(g(s\lambda_1), \dots, g(s\lambda_n))$ is the scaling matrix of the eigenvalues. The scaling function g takes the eigenvalue λ_i and an additional scaling factor s as inputs, indicating how a signal diffuses away from node i at scale s ; we select $g_s(\lambda) = \exp(-s\lambda)$ as the heat kernel. This means that we can vary the scaling parameter s to adjust the neighborhoods surrounding a center node. Please see 1 for more illustration. Following Ngo et al. [1], a set of k graph Wavelet $\{\psi\}_i^k \in \mathbb{R}^{n \times n}$ can be constructed to result in a tensor of graph Wavelet $\mathbf{W} \in \mathbb{R}^{n \times n \times k}$. Unlike structural encoding like random walk which only contains information at one hop length, Wavelets structural information decays gradually from each node to its neighborhood, and, thus, contains much more meaningful topological information.

Fast Graph Wavelet Transform. Traditionally, computing graph wavelet bases necessitates the full diagonalization of the graph Laplacian \tilde{L} in 1. This approach becomes computationally expensive when the number of nodes increases. Our work adopts the efficient algorithm proposed by Hammond et al. [21]. This method utilizes Chebyshev polynomials to approximate the Wavelet with a time complexity of $O(|E| \times M)$, where M represents the order of the polynomials and E is the set of edges. This approach scales linearly with the number of edges, thereby being more efficient than previous methods based on the eigendecomposition of the graph Laplacian.

4.2 Constructing Long-range Pretraining on Domain-Agnostic Data

Our goal is to train a learnable structural encoder to extract generalized and abstract node-level structural features that can be transferred across downstream tasks in graph learning. To fulfill this, we parameterize a high-order autoencoder [3–5, 15, 48] that learns to reconstruct high-order features of graph data from their wavelet tensors $\mathbf{W} \in \mathbb{R}^{n \times n \times k}$.

In particular, given a second-order wavelet tensor $\mathbf{W} \in \mathbb{R}^{n \times n \times k}$, the encoder \mathcal{E} encodes \mathbf{W} into a latent matrix $\mathbf{Z} = \mathcal{E}(\mathbf{W}) \in \mathbb{R}^{n \times d_e}$, the encoder \mathcal{E} can be composed of many equivariant operators. Furthermore, to reduce redundancy caused by high-order training, we extract only two equivariant



Pretrained Permutation Equivariant High-Order Autoencoder

Figure 2: Our proposed equivariant autoencoder pretraining scheme are applied on a large multiple domain dataset while extending the feature degree, overcoming the domain-specific weakness while also embedding long-range information.

mappings for the encoder, diagonal and row sum:

$$E_1(\mathbf{Z}) = \text{diag}(\mathbf{Z}), \quad E_2(\mathbf{Z}) = \mathbf{Z}\mathbf{1}_n.$$

Then, the decoder \mathcal{D} lifts \mathbf{Z} back to a high-order feature map $\mathcal{F} = \mathcal{D}(\mathbf{Z}) \in \mathbb{R}^{n \times n \times d}$. Here, We use the outer product and diagonal operator, which represent structural and positional informationn respectively:

$$D_1(\mathbf{Z}_i) = \mathbf{Z}_i \otimes \mathbf{Z}_i^\top, \quad D_2(\mathbf{Z}_i) = \text{diag}(\mathbf{Z}_i)$$

where \otimes is the outer product operator, and \mathbf{Z}_i is the i -th channel feature of the encoded information. Here, d_ℓ and d denote the channels (dimensions) of each entries in an $n \times n$ matrix.

Finally, we use a channel-wise multi-layer perceptron (MLP) $\phi: \mathbb{R}^{n \times n \times d} \mapsto \mathbb{R}^{n \times n \times r}$ to map \mathcal{F} to a concatenated high-degree adjacency matrix in binary values. Specifically, let \mathbf{A}_j be the binary matrix of j -hop neighbor in a graph and $\hat{\mathbf{A}}_j$ be its prediction. The final MLP network returns the predicted array

$$\phi(\mathbf{Z}) = [\hat{\mathbf{A}}_{s_1} \quad \hat{\mathbf{A}}_{s_2} \quad \dots \quad \hat{\mathbf{A}}_{s_r}], \quad (3)$$

where s_1, s_2, \dots, s_r are natural degrees to be chosen. In this work, we let these values follow a exponential pattern, which highlights the range-diversity.

Theoretically, we show that with sufficient budget, our pretraining schema can reach abitraily high accuracy, the full proof is provided at Appendix 4.

Theorem 1. For any $\epsilon > 0$ and real coefficients $\theta_1, \theta_2, \dots, \theta_d$, there exists a HOPE-WavePE $\varphi: \mathbb{R}^{n \times n \times d} \rightarrow \mathbb{R}^{n \times n}$ such that

$$\left\| \varphi(\mathbf{Z}) - \sum_{j=1}^r \theta_j \mathbf{A}_j \right\| < \epsilon.$$

Masking grants generalizability. In sparse structures, learning different hop adjacencies imposes disproportionality in edges and non-edges, which differs with the adjacency degree and also data structures. For example, a molecule graph from MoleculeNet [49] have shorter diameter than peptides [50]. Thus, long degree adjacency is redundant for small molecules and hurts the generalizability for bigger graphs. To fix this, we use a binary mask $\mathbf{M} \in \mathbb{R}^{n \times n \times r}$, filtering out random entries in both the ground truth and label such that non edges and edges are equal in quantity for each degree

of predicted adjacency. In particular, denote $\mathcal{M}(\mathbf{P})$ and $\mathcal{N}(\mathbf{P})$ as the number of non-zero and zero entries in matrix \mathbf{P} respectively, our formula for the masked value quantity is

$$\mathcal{M}(\mathbf{M}_i) = \min(\mathcal{M}(\mathbf{A}), \mathcal{N}(\mathbf{A}), \mathbf{T}), \quad (4)$$

where \mathbf{T} is some fixed threshold. The remaining entries define the binary cross entropy loss:

$$\mathcal{L}_{\mathbf{M}}(\mathbf{A}_{s_i}, \widehat{\mathbf{A}}_{s_i}) = \text{BinCrossEntropy}(\mathbf{M}_i \odot \mathbf{A}_{s_i}, \mathbf{M}_i \odot \widehat{\mathbf{A}}_{s_i}),$$

where \odot is the elementwise matrix product. There are two main motivations for this. **1)** Firstly, thresholding adjacency channels reduces training cost while keeping a fair learning quantity between hop lengths. **2)** Secondly, the masked AE can learn long hops for big graphs independently from smaller graphs which are masked out based on (4). This renders the autoencoder *range-awareness* of the input graph in downstream tasks and augment meaningful information to node features.

5 Experiments

This section empirically evaluates the advantages of our structurally pre-trained autoencoder (AE). We first detail the pre-training process, which utilizes a large dataset of graph structures. We then present experimental results on various downstream tasks. As our objective is to learn a structural feature extractor for graph data, we aim to demonstrate three key points:

- **Enhanced performance on small datasets:** The encoder of the pre-trained AE can extract structural features that enhance the performance of graph-level prediction tasks on small datasets.
- **Effective PSE feature representation:** The learned structural features can capture global information and preserve graph structures when integrated into and fine-tuned along with global models like graph transformers or VN-augmented MPNNs.
- **Generalizability:** The pre-trained AE can generalize well to out-of-distribution graphs with different connectivity types and sizes from the training dataset.

5.1 Setup

Pretraining. We pretrained a high-order autoencoder on MolPCBA [49] and Peptides-func [50]. During this pretraining stage, the autoencoder focuses on learning a set of topological hops, represented by the concatenated tensor $\{\mathbf{A}_{s_i}\}_{i=1}^r$. By excluding chemical features during pretraining, we granted the network versatility, enabling it to adapt to downstream tasks that use different feature representations. To incorporate multi-scale information, we constructed a 4-channel Wavelet tensor for each graph sample, with scaling factors of [1, 2, 4, 16]. The autoencoder architecture consisted of an encoder and a decoder, each containing three high-order linear layers. Another three-layer multilayer perceptron (MLP) was used to project the encoder’s output into a latent embedding of size 20. After being projected back by the decoder to generate new scaled wavelets, a MLP is used to learn the adjacency tensor $\{\mathbf{A}_{s_i}\}_{i=1}^r$. We divide the MolPCBA dataset into a train-valid ratio of 9:1 and use the prepared train-valid set for Peptides-func.

Downstream task. After pretraining, we integrated the pretrained autoencoder into other graph neural networks for graph-level supervised tasks. We concatenated the node-level structural features extracted by the pretrained autoencoder with domain-specific features before feeding them into GNN-based models for downstream evaluation. The implementation details for each specific downstream task are provided in Appendix B.

5.2 Results

While we pretrained our HOPE-WavePE autoencoder on the MolPCA and Peptides-func, the performance on downstream tasks within this benchmark may be limited to the chemical structures. To address this, we also evaluate HOPE-WavePE on a broader range of real-world graph datasets. These datasets encompass diverse graph structures, connectivity types, sizes, and domain-specific features, significantly differing from those found in molecules and peptides, highlighting how range-awareness adapt to extreme out-of-distribution (OOD) scenerios.

Table 1: Experimental results on five small molecule (scaffold-split) classification datasets. Methods are evaluated by ROC-AUC % (\uparrow) where higher scores mean better performances. We report the mean and standard deviation (in brackets) of all methods over three random seeds. Top 3 results are highlighted, including **First**, **Second**, and **Third**.

Method	BBBP	BACE	Tox21	ToxCast	SIDER
D-MPNN [51]	71.0(0.3)	80.9(0.6)	75.9(0.7)	65.5(0.3)	57.0(0.7)
AttentiveFP [52]	64.3(1.8)	78.4(0.0)	76.1(0.5)	63.7(0.2)	60.6(3.2)
N-GramRF [53]	69.7(0.6)	77.9(1.5)	74.3(0.4)	-	66.8(0.7)
N-GramXGB [53]	69.1(0.8)	79.1(1.3)	75.8(0.9)	-	65.5(0.7)
PretrainGNN [54]	68.7(1.3)	79.9(0.9)	76.7(0.4)	65.7(0.6)	62.7(0.8)
GROVERbase [55]	70.0(0.1)	82.6(0.7)	74.3(0.1)	65.4(0.4)	64.8(0.6)
GROVERlarge [55]	69.5(0.1)	81.0(1.4)	73.5(0.1)	65.3(0.5)	65.4(0.1)
GraphLOG pretrained [56]	72.5(0.8)	83.5(1.2)	75.7(0.5)	63.5(0.7)	61.2 (1.1)
GraphCL pretrained [57]	69.7(0.7)	75.4(1.4)	73.9(0.7)	62.4(0.6)	60.5(0.9)
InfoGraph pretrained [58]	66.3(0.6)	64.8(0.7)	68.1(0.6)	58.4(0.6)	57.1(0.8)
MPNN + HOPE-WavePE (ours)	71.2(0.4)	86.8(0.4)	78.0(0.1)	66.9(0.5)	64.7(0.3)

Moleculenet and Long Range Graph Benchmark. We first evaluate our encoding schema on the two data structures used for pretraining phase. In particular, we use scaffold splitting on five small molecule datasets from Moleculenet [49] and two datasets Peptides-func and Peptides-struct from Long Range Graph Benchmark (LRGB) [50], which are shown in Table 1 and 2. For Moleculenet, we compare our methods with multiple baselines, including supervised and pretraining. For LRGB, we compare our method against some standard message-passing neural networks and show that by augmenting using virtual node and HOPE-WavePE, they can outperform many Graph Transformer methods.

Table 2: Experimental results on Peptides func and Peptides struct. We report the means and standard deviations of 4 random seeds. The best results are highlighted **First**, **Second** and **Third**

Model	Peptides Struct MAE \downarrow	Peptides Func AP \uparrow
GCN [59]	0.3496 \pm 0.0013	0.5930 \pm 0.0023
GINE [6]	0.6346 \pm 0.0071	0.5498 \pm 0.0079
GatedGCN [60]	0.3420 \pm 0.0013	0.5864 \pm 0.0077
GatedGCN + RWSE [60]	0.3357 \pm 0.0006	0.6069 \pm 0.0035
Drew-GCN + LapPE [61]	0.2536 \pm 0.0015	0.7150 \pm 0.0044
GraphGPS + LapPE [34]	0.2500 \pm 0.0005	0.6535 \pm 0.0041
GRIT [19]	0.2460 \pm 0.0012	0.6988 \pm 0.0082
Graph VIT [62]	0.2449 \pm 0.0016	0.6942 \pm 0.0075
GraphMLP Mixer [62]	0.2475 \pm 0.0015	0.6921 \pm 0.0054
GatedGCN + VN + RWSE [13]	0.2529 \pm 0.0009	0.6685 \pm 0.0062
GatedGCN + VN + HOPE-WavePE (ours)	0.2433 \pm 0.0011	0.7171 \pm 0.0023

TUDataset Benchmark. We evaluate HOPE-WavePE on six diverse datasets from the TUDataset benchmark [63]: a small molecule dataset (MUTAG), two chemical compound datasets (NCI1 and NCI109), a macromolecule dataset (PROTEINS) and two social network datasets (IMDB-B and IMDB-M). In this task, we combine the structural features extracted by the pretrained autoencoder with node domain features and feed them into an MPNN consisting of five GIN [6] layers. The results in 3 demonstrate that GIN augmented with HOPE-WavePE significantly outperforms other complicated high-order networks like IGN [64], CIN, and PPGNs on three out of six datasets.

Different Graph Connectivity Patterns. We evaluate on two image classification datasets, MNIST and CIFAR-10 in [30]. In this task, we augment node superpixel features with their structural features before feeding them into GPS [34], a graph transformer model. As shown in 4, GPS + HOPE-WavePE achieves comparable accuracy to other MPNNs and GPS models that rely on different explicit positional encoding methods.

Table 3: Experimental results on TU datasets. The methods are evaluated by Accuracy % (\uparrow). The reported results are means and standard deviations of runnings over five random seeds. Top 3 results are highlighted, including **First**, **Second**, and **Third**.

Method	MUTAG	PROTEINS	NCI1	NCI109	IMDB-B	IMDB-M
RWK [65]	79.2 \pm 2.1	59.6 \pm 0.1	>3 days	-	-	-
GK ($k = 3$) [66]	81.4 \pm 1.7	71.4 \pm 0.3	62.5 \pm 0.3	62.4 \pm 0.3	-	-
PK [67]	76.0 \pm 2.7	73.7 \pm 0.7	82.5 \pm 0.5	-	-	-
WL kernel [68]	90.4 \pm 5.7	75.0 \pm 3.1	86.0 \pm 1.8	-	73.8 \pm 3.9	50.9 \pm 3.8
DCNN [69]	-	61.3 \pm 1.6	56.6 \pm 1.0	-	49.1 \pm 1.4	33.5 \pm 1.4
DGCNN [70]	85.8 \pm 1.8	75.5 \pm 0.9	74.4 \pm 0.5	-	70.0 \pm 0.9	47.8 \pm 0.9
IGN [64]	83.9 \pm 13.0	76.6 \pm 5.5	74.3 \pm 2.7	72.8 \pm 1.5	72.0 \pm 5.5	48.7 \pm 3.4
GIN [6]	89.4 \pm 5.6	76.2 \pm 2.8	82.7 \pm 1.7	-	75.1 \pm 5.1	52.3 \pm 2.8
PPGNs [71]	90.6 \pm 8.7	77.2 \pm 4.7	83.2 \pm 1.1	82.2 \pm 1.4	73.0 \pm 5.8	50.5 \pm 3.6
Natural GN [72]	89.4 \pm 1.6	71.7 \pm 1.0	82.4 \pm 1.3	-	73.5 \pm 2.0	51.3 \pm 1.5
GSN [73]	92.2 \pm 7.5	76.6 \pm 5.0	83.5 \pm 2.0	-	77.8 \pm 3.3	54.3 \pm 3.3
SIN [74]	-	76.4 \pm 3.3	82.7 \pm 2.1	-	75.6 \pm 3.2	52.4 \pm 2.9
CIN [75]	92.7 \pm 6.1	77.0 \pm 4.3	83.6 \pm 1.4	84.0 \pm 1.6	75.6 \pm 3.7	52.7 \pm 3.1
GIN + HOPE-WavePE (ours)	93.6 \pm 5.8	79.5 \pm 4.81	84.5 \pm 2.0	83.1 \pm 1.9	76.0 \pm 3.7	52.7 \pm 2.9

ZINC Dataset. We evaluate the performance of HOPE-WavePEs on a subset of the ZINC dataset [76] containing 12,000 graphs with up to 38 heavy atoms. We assess its ability to perform molecular tasks using GPS [34] equipped with HOPE-WavePE. The results in Table 4 our method outperforms the two most popular encoding baselines, LapPE and RWSE, and show statistically significant differences compared to traditional GNN methods.

Table 4: Experimental results on image classification tasks and ZINC. The results are reported by taking the mean \pm the std over four random seeds. Top 3 results are highlighted, including **First**, **Second** and **Third**.

Model	CIFAR10 ACC (%) \uparrow	MNIST ACC (%) \uparrow	ZINC MAE \downarrow
GIN [6]	55.26 \pm 1.53	96.49 \pm 0.25	0.526 \pm 0.051
GAT [77]	64.22 \pm 0.45	95.53 \pm 0.20	0.384 \pm 0.007
GatedGCN [60]	67.31 \pm 0.31	97.34 \pm 0.14	0.282 \pm 0.015
Graph MLP-Mixer [62]	72.46 \pm 0.36	98.35 \pm 0.10	0.077 \pm 0.003
GPS + none [78]	71.76 \pm 0.01	98.05 \pm 0.00	-
GPS + (RWSE/LapPE) [34]	72.30 \pm 0.36	98.05 \pm 0.13	0.070 \pm 0.004
GPS + HOPE-WavePE (ours)	73.01 \pm 0.81	98.15 \pm 0.11	0.067 \pm 0.002

5.3 Ablation Study

We have three focuses for our ablations. First, we explore how does the number of wavelet channels affect the reconstructability of the adjacency tensor. Secondly, we show that cross-domain training only improve performance incrementally. And finally, we show how masked and unmasked training affect the reconstructability of HOPE-WavePE on medium-sized graphs.

Wavelet Channel Number. As shown in Figure 1, different scaling factors impact the receptive field of each node. Since each resolution is responsible for learning a specific range of hops, more multiresolutions should capture diverse-range dependency. We visualize in Figure 3 by recording the reconstruction accuracies of the concatenated array $\{\mathbf{A}_{2^i}\}_{i=0}^7$ given 7, 10, 20, 30 and 60 wavelet channels respectively. The experiment is conducted on the peptides-struct dataset from the Long Range Graph Benchmark [50], which highlights the long-range learnability.

Cross-Domain Training. To further verify transferability of HOPE-WavePE onto different tasks in a direct manner, we train HOPE-WavePE on four different datasets with great domain disparity, namely: ZINC (molecule), MNIST (image), ogbl-collab (collaborative network) and ogbl-ppa (interaction network), and record the decoded accuracy on the reconstruction the adjacency matrix. To avoid resource insufficiency in processing the two ogbl tasks while not changing their intrinsic

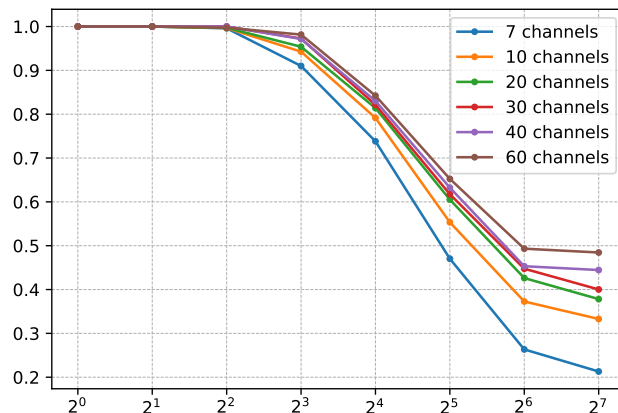


Figure 3: Average reconstruction accuracy on Peptides-struct graphs with different wavelet channel quantities.

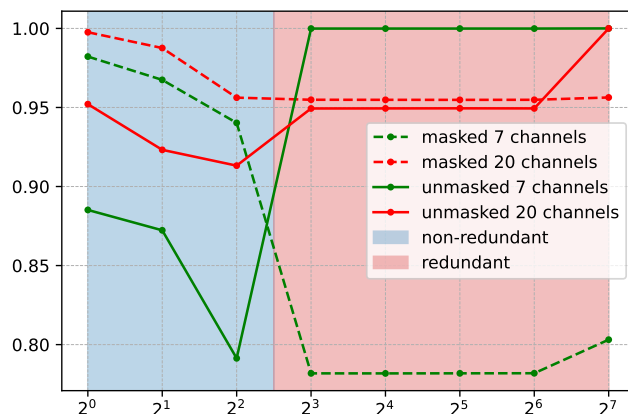


Figure 4: Masked vs unmasked reconstruction accuracy on MNIST dataset. The regions shaded **red** and **blue** contains hop lengths s in which \mathbf{A}_s are and are not all ones, respectively.

structure, we partitioned them into almost similar size graphs as in MNIST and ZINC using METIS algorithm. Our results shown in Table 5 indicates the transferrability of HOPE-WavePE to extremely different domains, given that their sizes are similar.

Table 5: Accuracy of HOPE-WavePE on cross-domain training.

Domain Type	Name	ZINC	MNIST	ogbl-collab	ogbl-ppa
Molecular	ZINC	0.9891	0.9734	0.9812	0.9734
Image	MNIST	0.9652	0.9753	0.9652	0.9712
Collaborative Network	ogbl-collab	0.9860	0.9860	0.9742	0.9812
Interaction Network	ogbl-ppa	0.9767	0.9767	0.9832	0.9912

Masked vs Unmasked. To visually illustrate our motivation of masking the autoencoder, we evaluated HOPE-WavePE on reconstructing the concatenated adjacency $\{\mathbf{A}_{2^i}\}_{i=0}^7$ over the MNIST dataset. Note that, these graphs are connected and their diameter is far below the considered range. In particular, $\mathbf{A}_s = \mathbf{1}_{n \times n}$ for all $s \geq 8$, and, thus, are redundant in the structural learning. From Figure 4, we see that masking significantly removes redundant learning from exceedingly long range, which would punishes important ranges otherwise.

6 Conclusion

We have introduced HOPE-WavePE, a novel high-order permutation-equivariant pretraining method specifically designed for graph-structured data. Our approach leverages the inherent connectivity of graphs, eliminating reliance on domain-specific features while being range-aware. This enables HOPE-WavePE to generalize effectively across diverse graph types and domains. The superiority of HOPE-WavePE is demonstrably proven through both theoretical and empirical analysis. Finally, we have discussed the potential of HOPE-WavePE as a foundation for a general graph structural encoder. A promising future direction will be to focus on optimizing the scalability of this approach.

References

- [1] Nhat Khang Ngo, Truong Son Hy, and Risi Kondor. Multiresolution graph transformers and wavelet positional encoding for learning long-range and hierarchical structures. *The Journal of Chemical Physics*, 159(3):034109, 07 2023. ISSN 0021-9606. doi: 10.1063/5.0152833. URL <https://doi.org/10.1063/5.0152833>. 1, 2, 3, 4
- [2] Truong Son Hy. Graph representation learning, deep generative models on graphs, group equivariant molecular neural networks and multiresolution machine learning. page 366. doi: <https://doi.org/10.6082/uchicago.4761>. URL <http://knowledge.uchicago.edu/record/4761>. 1
- [3] Erik Henning Thiede, Truong Son Hy, and Risi Kondor. The general theory of permutation equivariant neural networks and higher order graph variational encoders. *arXiv preprint arXiv:2004.03990*, 2020. 4
- [4] Truong Son Hy, Shubhendu Trivedi, Horace Pan, Brandon M. Anderson, and Risi Kondor. Predicting molecular properties with covariant compositional networks. *The Journal of Chemical Physics*, 148(24):241745, 06 2018. ISSN 0021-9606. doi: 10.1063/1.5024797. URL <https://doi.org/10.1063/1.5024797>.
- [5] Truong Son Hy, Shubhendu Trivedi, Horace Pan, Brandon M Anderson, and Risi Kondor. Covariant compositional networks for learning graphs. In *Proc. International Workshop on Mining and Learning with Graphs (MLG)*, 2019. 4
- [6] Keyulu Xu, Weihua Hu, Jure Leskovec, and Stefanie Jegelka. How powerful are graph neural networks? In *7th International Conference on Learning Representations, ICLR 2019, New Orleans, LA, USA, May 6-9, 2019*. OpenReview.net, 2019. URL <https://openreview.net/forum?id=ryGs6iA5Km>. 1, 7, 8
- [7] Deli Chen, Yankai Lin, Wei Li, Peng Li, Jie Zhou, and Xu Sun. Measuring and relieving the over-smoothing problem for graph neural networks from the topological view. *Proceedings of the AAAI Conference on Artificial Intelligence*, 34(04):3438–3445, Apr. 2020. doi: 10.1609/aaai.v34i04.5747. URL <https://ojs.aaai.org/index.php/AAAI/article/view/5747>. 1
- [8] Jake Topping, Francesco Di Giovanni, Benjamin Paul Chamberlain, Xiaowen Dong, and Michael M. Bronstein. Understanding over-squashing and bottlenecks on graphs via curvature. In *International Conference on Learning Representations*, 2022. URL <https://openreview.net/forum?id=7UmjRGzp-A>. 1
- [9] Seongjun Yun, Minbyul Jeong, Raehyun Kim, Jaewoo Kang, and Hyunwoo J Kim. Graph transformer networks. In H. Wallach, H. Larochelle, A. Beygelzimer, F. d'Alché-Buc, E. Fox, and R. Garnett, editors, *Advances in Neural Information Processing Systems*, volume 32. Curran Associates, Inc., 2019. URL <https://proceedings.neurips.cc/paper/2019/file/9d63484abb477c97640154d40595a3bb-Paper.pdf>. 1, 2, 3
- [10] Devin Kreuzer, Dominique Beaini, Will Hamilton, Vincent Létourneau, and Prudencio Tossou. Rethinking graph transformers with spectral attention. In M. Ranzato, A. Beygelzimer, Y. Dauphin, P.S. Liang, and J. Wortman Vaughan, editors, *Advances in Neural Information Processing Systems*, volume 34, pages 21618–21629. Curran Associates, Inc., 2021. URL https://proceedings.neurips.cc/paper_files/paper/2021/file/b4fd1d2cb085390fbbadae65e07876a7-Paper.pdf. 3
- [11] Vijay Prakash Dwivedi and Xavier Bresson. A generalization of transformer networks to graphs. *CoRR*, abs/2012.09699, 2020. URL <https://arxiv.org/abs/2012.09699>. 2

- [12] Chengxuan Ying, Tianle Cai, Shengjie Luo, Shuxin Zheng, Guolin Ke, Di He, Yanming Shen, and Tie-Yan Liu. Do transformers really perform badly for graph representation? In A. Beygelzimer, Y. Dauphin, P. Liang, and J. Wortman Vaughan, editors, *Advances in Neural Information Processing Systems*, 2021. URL <https://openreview.net/forum?id=0eWooOxFwDa>. 1
- [13] Chen Cai, Truong Son Hy, Rose Yu, and Yusu Wang. On the connection between mpnn and graph transformer. *arXiv preprint arXiv:2301.11956*, 2023. 1, 2, 7, 19
- [14] Thuan Nguyen Anh Trang, Khang Nhat Ngo, Hugo Sonnery, Thieu Vo, Siamak Ravanbakhsh, and Truong Son Hy. Scalable hierarchical self-attention with learnable hierarchy for long-range interactions. *Transactions on Machine Learning Research*, 2024. ISSN 2835-8856. URL <https://openreview.net/forum?id=qH4YFMyhce>.
- [15] Truong Son Hy and Risi Kondor. Multiresolution equivariant graph variational autoencoder. *Machine Learning: Science and Technology*, 4(1):015031, mar 2023. doi: 10.1088/2632-2153/acc0d8. URL <https://dx.doi.org/10.1088/2632-2153/acc0d8>. 1, 2, 4
- [16] Zhishang Luo, Truong Son Hy, Puoya Tabaghi, Michaël Defferrard, Elahe Rezaei, Ryan M. Carey, Rhett Davis, Rajeev Jain, and Yusu Wang. DE-HNN: An effective neural model for circuit Netlist representation. In Sanjoy Dasgupta, Stephan Mandt, and Yingzhen Li, editors, *Proceedings of The 27th International Conference on Artificial Intelligence and Statistics*, volume 238 of *Proceedings of Machine Learning Research*, pages 4258–4266. PMLR, 02–04 May 2024. URL <https://proceedings.mlr.press/v238/luo24a.html>.
- [17] Justin Gilmer, Samuel S. Schoenholz, Patrick F. Riley, Oriol Vinyals, and George E. Dahl. Neural message passing for quantum chemistry. In *Proceedings of the 34th International Conference on Machine Learning - Volume 70*, ICML’17, page 1263–1272. JMLR.org, 2017. 2
- [18] Vijay Prakash Dwivedi, Anh Tuan Luu, Thomas Laurent, Yoshua Bengio, and Xavier Bresson. Graph neural networks with learnable structural and positional representations. In *International Conference on Learning Representations*, 2022. URL <https://openreview.net/forum?id=wTTjnvGphYj>. 2, 3
- [19] Liheng Ma, Chen Lin, Derek Lim, Adriana Romero-Soriano, K. Dokania, Mark Coates, Philip H.S. Torr, and Ser-Nam Lim. Graph Inductive Biases in Transformers without Message Passing. In *Proc. Int. Conf. Mach. Learn.*, 2023. 2, 3, 7
- [20] Bingbing Xu, Huawei Shen, Qi Cao, Yunqi Qiu, and Xueqi Cheng. Graph wavelet neural network. In *International Conference on Learning Representations*, 2019. URL <https://openreview.net/forum?id=H1ewdiR5tQ>. 2
- [21] David K Hammond, Pierre Vandergheynst, and Rémi Gribonval. Wavelets on graphs via spectral graph theory. *Applied and Computational Harmonic Analysis*, 30(2):129–150, 2011. 4
- [22] Claire Donnat, Marinka Zitnik, David Hallac, and Jure Leskovec. Learning structural node embeddings via diffusion wavelets. In *Proceedings of the 24th ACM SIGKDD International Conference on Knowledge Discovery & Data Mining*, KDD ’18, page 1320–1329, New York, NY, USA, 2018. Association for Computing Machinery. ISBN 9781450355520. doi: 10.1145/3219819.3220025. URL <https://doi.org/10.1145/3219819.3220025>.
- [23] Truong Son Hy and Risi Kondor. Multiresolution matrix factorization and wavelet networks on graphs. In Alexander Cloninger, Timothy Doster, Tegan Emerson, Manohar Kaul, Ira Ktena, Henry Kvinge, Nina Miolane, Bastian Rieck, Sarah Tymochko, and Guy Wolf, editors, *Proceedings of Topological, Algebraic, and Geometric Learning Workshops 2022*, volume 196 of *Proceedings of Machine Learning Research*, pages 172–182. PMLR, 25 Feb–22 Jul 2022. URL <https://proceedings.mlr.press/v196/hy22a.html>. 2
- [24] Duc Thien Nguyen, Manh Tuan Nguyen, Truong Son Hy, and Risi Kondor. Fast temporal wavelet graph neural networks. In Sophia Sanborn, Christian Shewmake, Simone Azeglio, and Nina Miolane, editors, *Proceedings of the 2nd NeurIPS Workshop on Symmetry and Geometry in Neural Representations*, volume 228 of *Proceedings of Machine Learning Research*, pages 35–54. PMLR, 16 Dec 2024. URL <https://proceedings.mlr.press/v228/nguyen24a.html>. 2
- [25] Sinno Jialin Pan and Qiang Yang. A survey on transfer learning. *IEEE Transactions on Knowledge and Data Engineering*, 22(10):1345–1359, 2010. doi: 10.1109/TKDE.2009.191. 2

- [26] Dan Hendrycks, Kimin Lee, and Mantas Mazeika. Using pre-training can improve model robustness and uncertainty. In Kamalika Chaudhuri and Ruslan Salakhutdinov, editors, *Proceedings of the 36th International Conference on Machine Learning*, volume 97 of *Proceedings of Machine Learning Research*, pages 2712–2721. PMLR, 09–15 Jun 2019. URL <https://proceedings.mlr.press/v97/hendrycks19a.html>. 2
- [27] Marinka Zitnik, Rok Sosič, and Jure Leskovec. Prioritizing network communities. *Nature Communications*, 9(1):2544, Jun 2018. ISSN 2041-1723. doi: 10.1038/s41467-018-04948-5. URL <https://doi.org/10.1038/s41467-018-04948-5>. 2
- [28] Derek Lim, Joshua Robinson, Lingxiao Zhao, Tess Smidt, Suvrit Sra, Haggai Maron, and Stefanie Jegelka. Sign and basis invariant networks for spectral graph representation learning, 2022. 2
- [29] Haorui Wang, Haoteng Yin, Muhan Zhang, and Pan Li. Equivariant and stable positional encoding for more powerful graph neural networks. In *International Conference on Learning Representations*, 2022. URL <https://openreview.net/forum?id=e95i1IHcWj>. 3
- [30] Vijay Prakash Dwivedi, Chaitanya K. Joshi, Anh Tuan Luu, Thomas Laurent, Yoshua Bengio, and Xavier Bresson. Benchmarking graph neural networks. *Journal of Machine Learning Research*, 24(43):1–48, 2023. URL <http://jmlr.org/papers/v24/22-0567.html>. 2, 7
- [31] Vijay Prakash Dwivedi and Xavier Bresson. A generalization of transformer networks to graphs. *CoRR*, abs/2012.09699, 2020. URL <https://arxiv.org/abs/2012.09699>. 2, 3
- [32] Romain Menegaux, Emmanuel Jehanno, Margot Selosse, and Julien Mairal. Self-attention in colors: Another take on encoding graph structure in transformers. *Transactions on Machine Learning Research*, 2023. ISSN 2835-8856. URL <https://openreview.net/forum?id=3dQCNqqv2d>.
- [33] Jinwoo Kim, Dat Nguyen, Seonwoo Min, Sungjun Cho, Moontae Lee, Honglak Lee, and Seunghoon Hong. Pure transformers are powerful graph learners. In S. Koyejo, S. Mohamed, A. Agarwal, D. Belgrave, K. Cho, and A. Oh, editors, *Advances in Neural Information Processing Systems*, volume 35, pages 14582–14595. Curran Associates, Inc., 2022. URL https://proceedings.neurips.cc/paper_files/paper/2022/file/5d84236751fe6d25dc06db055a3180b0-Paper-Conference.pdf. 3
- [34] Ladislav Rampásek, Mikhail Galkin, Vijay Prakash Dwivedi, Anh Tuan Luu, Guy Wolf, and Dominique Beaini. Recipe for a General, Powerful, Scalable Graph Transformer. *arXiv:2205.12454*, 2022. 2, 3, 7, 8, 19
- [35] Grégoire Mialon, Dexiong Chen, Margot Selosse, and Julien Mairal. Graphit: Encoding graph structure in transformers. *arXiv preprint arXiv:2106.05667*, 2021. 3
- [36] Pan Li, Yanbang Wang, Hongwei Wang, and Jure Leskovec. Distance encoding: Design provably more powerful neural networks for graph representation learning. *Advances in Neural Information Processing Systems*, 33, 2020. 3
- [37] Chengxuan Ying, Tianle Cai, Shengjie Luo, Shuxin Zheng, Guolin Ke, Di He, Yanming Shen, and Tie-Yan Liu. Do transformers really perform badly for graph representation? In M. Ranzato, A. Beygelzimer, Y. Dauphin, P.S. Liang, and J. Wortman Vaughan, editors, *Advances in Neural Information Processing Systems*, volume 34, pages 28877–28888. Curran Associates, Inc., 2021. URL https://proceedings.neurips.cc/paper_files/paper/2021/file/f1c1592588411002af340cbaedd6fc33-Paper.pdf. 3
- [38] Renming Liu, Semih Cantürk, Olivier Lapointe-Gagné, Vincent Létourneau, Guy Wolf, Dominique Beaini, and Ladislav Rampásek. Graph positional and structural encoder. *arXiv preprint arXiv:2307.07107*, 2023. 3
- [39] Tom Brown, Benjamin Mann, Nick Ryder, Melanie Subbiah, Jared D Kaplan, Prafulla Dhariwal, Arvind Neelakantan, Pranav Shyam, Girish Sastry, Amanda Askell, et al. Language models are few-shot learners. *Advances in neural information processing systems*, 33:1877–1901, 2020. 3
- [40] Gemini Team, Rohan Anil, Sebastian Borgeaud, Yonghui Wu, Jean-Baptiste Alayrac, Jiahui Yu, Radu Soricut, Johan Schalkwyk, Andrew M Dai, Anja Hauth, et al. Gemini: a family of highly capable multimodal models. *arXiv preprint arXiv:2312.11805*, 2023. 3
- [41] Kaiming He, Haoqi Fan, Yuxin Wu, Saining Xie, and Ross Girshick. Momentum contrast for unsupervised visual representation learning. In *Proceedings of the IEEE/CVF conference on computer vision and pattern recognition*, pages 9729–9738, 2020. 3

- [42] Alec Radford, Jong Wook Kim, Chris Hallacy, Aditya Ramesh, Gabriel Goh, Sandhini Agarwal, Girish Sastry, Amanda Askell, Pamela Mishkin, Jack Clark, et al. Learning transferable visual models from natural language supervision. In *International conference on machine learning*, pages 8748–8763. PMLR, 2021. 3
- [43] Yuning You, Tianlong Chen, Yang Shen, and Zhangyang Wang. Graph contrastive learning automated. In Marina Meila and Tong Zhang, editors, *Proceedings of the 38th International Conference on Machine Learning*, volume 139 of *Proceedings of Machine Learning Research*, pages 12121–12132. PMLR, 18–24 Jul 2021. URL <https://proceedings.mlr.press/v139/you21a.html>. 3
- [44] Minghao Xu, Hang Wang, Bingbing Ni, Hongyu Guo, and Jian Tang. Self-supervised graph-level representation learning with local and global structure. In Marina Meila and Tong Zhang, editors, *Proceedings of the 38th International Conference on Machine Learning*, volume 139 of *Proceedings of Machine Learning Research*, pages 11548–11558. PMLR, 18–24 Jul 2021. URL <https://proceedings.mlr.press/v139/xu21g.html>.
- [45] Yanqiao Zhu, Yichen Xu, Qiang Liu, and Shu Wu. An empirical study of graph contrastive learning. *arXiv preprint arXiv:2109.01116*, 2021.
- [46] Yuning You, Tianlong Chen, Yongduo Sui, Ting Chen, Zhangyang Wang, and Yang Shen. Graph contrastive learning with augmentations. In H. Larochelle, M. Ranzato, R. Hadsell, M. F. Balcan, and H. Lin, editors, *Advances in Neural Information Processing Systems*, volume 33, pages 5812–5823. Curran Associates, Inc., 2020. URL <https://proceedings.neurips.cc/paper/2020/file/3fe230348e9a12c13120749e3f9fa4cd-Paper.pdf>.
- [47] Yizhu Jiao, Yun Xiong, Jiawei Zhang, Yao Zhang, Tianqi Zhang, and Yangyong Zhu. Sub-graph contrast for scalable self-supervised graph representation learning. In *2020 IEEE international conference on data mining (ICDM)*, pages 222–231. IEEE, 2020. 3
- [48] Risi Kondor, Hy Truong Son, Horace Pan, Brandon Anderson, and Shubhendu Trivedi. Covariant compositional networks for learning graphs. *arXiv preprint arXiv:1801.02144*, 2018. 4
- [49] Zhenqin Wu, Bharath Ramsundar, Evan N Feinberg, Joseph Gomes, Caleb Geniesse, Aneesh S Pappu, Karl Leswing, and Vijay Pande. Moleculenet: a benchmark for molecular machine learning. *Chemical science*, 9(2):513–530, 2018. 5, 6, 7
- [50] Vijay Prakash Dwivedi, Ladislav Rampasek, Mikhail Galkin, Ali Parviz, Guy Wolf, Anh Tuan Luu, and Dominique Beaini. Long range graph benchmark. In *Thirty-sixth Conference on Neural Information Processing Systems Datasets and Benchmarks Track*, 2022. URL <https://openreview.net/forum?id=in7XC5RcjEn>. 5, 6, 7, 8
- [51] Kevin Yang, Kyle Swanson, Wengong Jin, Connor Coley, Philipp Eiden, Hua Gao, Angel Guzman-Perez, Timothy Hopper, Brian Kelley, Miriam Mathea, et al. Analyzing learned molecular representations for property prediction. *Journal of chemical information and modeling*, 59(8):3370–3388, 2019. 7
- [52] Zhaoping Xiong, Dingyan Wang, Xiaohong Liu, Feisheng Zhong, Xiaozhe Wan, Xutong Li, Zhaojun Li, Xiaomin Luo, Kaixian Chen, Hualiang Jiang, et al. Pushing the boundaries of molecular representation for drug discovery with the graph attention mechanism. *Journal of medicinal chemistry*, 63(16):8749–8760, 2019. 7
- [53] Shengchao Liu, Mehmet F Demirel, and Yingyu Liang. N-gram graph: Simple unsupervised representation for graphs, with applications to molecules. In H. Wallach, H. Larochelle, A. Beygelzimer, F. d’Alché-Buc, E. Fox, and R. Garnett, editors, *Advances in Neural Information Processing Systems*, volume 32. Curran Associates, Inc., 2019. URL https://proceedings.neurips.cc/paper_files/paper/2019/file/2f3926f0a9613f3c3cc21d52a3cdb4d9-Paper.pdf. 7
- [54] Weihua Hu, Bowen Liu, Joseph Gomes, Marinka Zitnik, Percy Liang, Vijay Pande, and Jure Leskovec. Strategies for pre-training graph neural networks. In *International Conference on Learning Representations*, 2020. URL <https://openreview.net/forum?id=HJ1WJJSFDH>. 7
- [55] Yu Rong, Yatao Bian, Tingyang Xu, Weiyang Xie, Ying Wei, Wenbing Huang, and Junzhou Huang. Self-supervised graph transformer on large-scale molecular data. In *Proceedings of the*

- 34th International Conference on Neural Information Processing Systems*, NIPS'20, Red Hook, NY, USA, 2020. Curran Associates Inc. ISBN 9781713829546. 7
- [56] Minghao Xu, Hang Wang, Bingbing Ni, Hongyu Guo, and Jian Tang. Self-supervised graph-level representation learning with local and global structure. In Marina Meila and Tong Zhang, editors, *Proceedings of the 38th International Conference on Machine Learning*, volume 139 of *Proceedings of Machine Learning Research*, pages 11548–11558. PMLR, 18–24 Jul 2021. URL <https://proceedings.mlr.press/v139/xu21g.html>. 7
- [57] Yuning You, Tianlong Chen, Yongduo Sui, Ting Chen, Zhangyang Wang, and Yang Shen. Graph contrastive learning with augmentations. In H. Larochelle, M. Ranzato, R. Hadsell, M.F. Balcan, and H. Lin, editors, *Advances in Neural Information Processing Systems*, volume 33, pages 5812–5823. Curran Associates, Inc., 2020. URL https://proceedings.neurips.cc/paper_files/paper/2020/file/3fe230348e9a12c13120749e3f9fa4cd-Paper.pdf. 7
- [58] Hanchen Wang, Jean Kaddour, Shengchao Liu, Jian Tang, Joan Lasenby, and Qi Liu. Evaluating self-supervised learning for molecular graph embeddings. In A. Oh, T. Naumann, A. Globerson, K. Saenko, M. Hardt, and S. Levine, editors, *Advances in Neural Information Processing Systems*, volume 36, pages 68028–68060. Curran Associates, Inc., 2023. URL https://proceedings.neurips.cc/paper_files/paper/2023/file/d6dc15cc2442a40904e704d624d1f8e8-Paper-Datasets_and_Benchmarks.pdf. 7
- [59] Thomas N Kipf and Max Welling. Semi-supervised classification with graph convolutional networks. *arXiv preprint arXiv:1609.02907*, 2016. 7
- [60] Xavier Bresson and Thomas Laurent. Residual gated graph convnets. *CoRR*, abs/1711.07553, 2017. URL <http://arxiv.org/abs/1711.07553>. 7, 8
- [61] Benjamin Gutteridge, Xiaowen Dong, Michael Bronstein, and Francesco Di Giovanni. Draw: Dynamically rewired message passing with delay, 2023. 7
- [62] Xiaoxin He, Bryan Hooi, Thomas Laurent, Adam Perold, Yann LeCun, and Xavier Bresson. A generalization of vit/mlp-mixer to graphs, 2023. 7, 8
- [63] Christopher Morris, Nils M Kriege, Franka Bause, Kristian Kersting, Petra Mutzel, and Marion Neumann. Tudataset: A collection of benchmark datasets for learning with graphs. *arXiv preprint arXiv:2007.08663*, 2020. 7
- [64] Haggai Maron, Heli Ben-Hamu, Nadav Shami, and Yaron Lipman. Invariant and equivariant graph networks. In *International Conference on Learning Representations*, 2019. URL <https://openreview.net/forum?id=Syx72jC9tm>. 7, 8, 18
- [65] Thomas Gärtner, Peter Flach, and Stefan Wrobel. On graph kernels: Hardness results and efficient alternatives. In Bernhard Schölkopf and Manfred K. Warmuth, editors, *Learning Theory and Kernel Machines*, pages 129–143, Berlin, Heidelberg, 2003. Springer Berlin Heidelberg. ISBN 978-3-540-45167-9. 8
- [66] Nino Shervashidze, SVN Vishwanathan, Tobias Petri, Kurt Mehlhorn, and Karsten Borgwardt. Efficient graphlet kernels for large graph comparison. In David van Dyk and Max Welling, editors, *Proceedings of the Twelfth International Conference on Artificial Intelligence and Statistics*, volume 5 of *Proceedings of Machine Learning Research*, pages 488–495, Hilton Clearwater Beach Resort, Clearwater Beach, Florida USA, 16–18 Apr 2009. PMLR. URL <https://proceedings.mlr.press/v5/shervashidze09a.html>. 8
- [67] Marion Neumann, R. Garnett, Christian Bauckhage, and Kristian Kersting. Propagation kernels: efficient graph kernels from propagated information. *Machine Learning*, 102:209 – 245, 2014. URL <https://api.semanticscholar.org/CorpusID:14487732>. 8
- [68] Nino Shervashidze, Pascal Schweitzer, Erik Jan van Leeuwen, Kurt Mehlhorn, and Karsten M. Borgwardt. Weisfeiler-lehman graph kernels. *Journal of Machine Learning Research*, 12(77): 2539–2561, 2011. URL <http://jmlr.org/papers/v12/shervashidze11a.html>. 8
- [69] James Atwood and Don Towsley. Diffusion-convolutional neural networks, 2016. 8
- [70] Muhan Zhang, Zhicheng Cui, Marion Neumann, and Yixin Chen. An end-to-end deep learning architecture for graph classification. In *Proceedings of the Thirty-Second AAAI Conference on Artificial Intelligence and Thirtieth Innovative Applications of Artificial Intelligence Conference and Eighth AAAI Symposium on Educational Advances in Artificial Intelligence*, AAAI'18/IAAI'18/EAAI'18. AAAI Press, 2018. ISBN 978-1-57735-800-8. 8

- [71] Haggai Maron, Heli Ben-Hamu, Hadar Serviansky, and Yaron Lipman. Provably powerful graph networks. In H. Wallach, H. Larochelle, A. Beygelzimer, F. d'Alché-Buc, E. Fox, and R. Garnett, editors, *Advances in Neural Information Processing Systems*, volume 32. Curran Associates, Inc., 2019. URL <https://proceedings.neurips.cc/paper/2019/file/bb04af0f7ecaee4aae62035497da1387-Paper.pdf>. 8
- [72] Pim de Haan, Taco Cohen, and Max Welling. Natural graph networks, 2020. 8
- [73] Giorgos Bouritsas, Fabrizio Frasca, Stefanos Zafeiriou, and Michael M. Bronstein. Improving graph neural network expressivity via subgraph isomorphism counting. *IEEE Transactions on Pattern Analysis and Machine Intelligence*, 45(1):657–668, 2023. doi: 10.1109/TPAMI.2022.3154319. 8
- [74] Cristian Bodnar, Fabrizio Frasca, Yu Guang Wang, Nina Otter, Guido Montúfar, Pietro Liò, and Michael Bronstein. Weisfeiler and lehman go topological: Message passing simplicial networks, 2021. 8
- [75] Cristian Bodnar, Fabrizio Frasca, Nina Otter, Yu Guang Wang, Pietro Liò, Guido Montúfar, and Michael Bronstein. Weisfeiler and lehman go cellular: Cw networks, 2022. 8, 19
- [76] Rafael Gómez-Bombarelli, David Duvenaud, José Miguel Hernández-Lobato, Jorge Aguilera-Iparraguirre, Timothy D. Hirzel, Ryan P. Adams, and Alán Aspuru-Guzik. Automatic chemical design using a data-driven continuous representation of molecules. *CoRR*, abs/1610.02415, 2016. URL <http://arxiv.org/abs/1610.02415>. 8
- [77] Petar Veličković, Guillem Cucurull, Arantxa Casanova, Adriana Romero, Pietro Liò, and Yoshua Bengio. Graph Attention Networks. *International Conference on Learning Representations*, 2018. URL <https://openreview.net/forum?id=rJXMpikCZ>. 8
- [78] Semih Cantürk, Renming Liu, Olivier Lapointe-Gagné, Vincent Létourneau, Guy Wolf, Dominique Beaini, and Ladislav Rampášek. Graph positional and structural encoder, 2024. URL <https://arxiv.org/abs/2307.07107>. 8
- [79] Espen Sande, Carla Manni, and Hendrik Speleers. Explicit error estimates for spline approximation of arbitrary smoothness in isogeometric analysis. *Numerische Mathematik*, 144(4):889–929, January 2020. ISSN 0945-3245. doi: 10.1007/s00211-019-01097-9. URL <http://dx.doi.org/10.1007/s00211-019-01097-9>. 16
- [80] Michaël Defferrard, Lionel Martin, Rodrigo Pena, and Nathanaël Perraudin. Pygsp: Graph signal processing in python. URL <https://github.com/epfl-lts2/pygsp>, 2017. 18
- [81] Yunsheng Shi, Zhengjie Huang, Shikun Feng, Hui Zhong, Wenjing Wang, and Yu Sun. Masked label prediction: Unified message passing model for semi-supervised classification. In Zhi-Hua Zhou, editor, *Proceedings of the Thirtieth International Joint Conference on Artificial Intelligence, IJCAI-21*, pages 1548–1554. International Joint Conferences on Artificial Intelligence Organization, 8 2021. doi: 10.24963/ijcai.2021/214. URL <https://doi.org/10.24963/ijcai.2021/214>. Main Track. 18

A Theoretical analysis

Notations. Throughout this section, for $\mathbf{X} \in \mathbb{R}^{m \times n}$, we denote $\mathbf{X}[i : j]$ as the indexed matrix of X from row i to row j and $X[i]$ as the i -th row of \mathbf{X} .

A.1 Preliminary results

The approximation methodology we use is the spline approximation on the eigenvalues of the laplacians, which later . First we need to define a scalar k -spline function on a bounded domain $[a, b] \subset \mathbb{R}$. Let

$$a =: \eta_1 < \eta_2 < \dots < \eta_{N+1} := b$$

such that $\eta_{j+1} = \eta_j + (b - a)/N$, these points are called uniform knots in the interval $[a, b]$. Assume that \mathcal{P}_k is the class of polynomial up degree at most k .

Definition 2. A scalar function f is called a k -spline function in the uniformly-divided interval $[a, b]$ of $N + 1$ knots if the follows conditions are satisfied:

- $f(x) = p_i(x) \quad \forall x \in [\eta_i, \eta_{i+1}], i = \overline{1, N}$ for some $p_i \in \mathcal{P}_k$,
- Derivative of f up to degree k is continuous.

For convenience, we denote the class of all such functions in Definition 2 as $\mathcal{S}_{k,N}^{[a,b]}$.

Lemma 1. (spline approximation power) [79] Given a scalar function u of smoothness order $k + 1$ in the range $[a, b]$ divided in uniform knots of length h , there exists $p \in \mathcal{S}_{k,N}^{[a,b]}$ such that

$$\|u - p\| \leq \left(\frac{h}{\pi}\right)^k \|u^{(k+1)}\|$$

where $u^{(k+1)}$ is the $(k + 1)$ -th order derivative of u .

Our proof strategy incorporate the approximation of high degree polynomial with k -spline methodology. Since both wavelet and random walk second feature embeddings' largest eigenvalue is 1 and smallest eigenvalue is -1, we can let $a = -1$ and $b = 1$ in our case. Note that in a two-layer MLP, the number of subintervals $[\eta_i, \eta_{i+1}]$ should correspond to the width in the hidden layer, which is equivalent to $1/h$. Therefore, Lemma 1 yields the condition in which a tolerance ϵ is satisfied.

Letting $u(x) = x^d$ for some $d > k$, then u is obviously smooth up to arbitrary order, thus it is also smooth of order k . We will let $\|\cdot\|$ be the max norm in the interval $[0, 1]$, then we have

$$\|u^{(k+1)}\|^{1/k} = (d(d-1) \dots (d-k))^{1/k} \sup_{x \in [0,1]} x^{\frac{d-k+1}{k}} \leq d^{1+\frac{1}{k}}$$

Combine this with the statement of Lemma 1 we deduce that the error defined by the max norm will be less than ϵ if

$$w := \frac{1}{h} \geq \pi^{-1} \epsilon^{-\frac{1}{k}} d^{1+\frac{1}{k}} = O\left(\epsilon^{-\frac{1}{k}} d^{1+\frac{1}{k}}\right).$$

From here, we deduce an important lemma:

Lemma 2. Given two natural numbers d and k such that $d > k$, then there exists a two-layer MLP $f : \mathbb{R}^k \rightarrow \mathbb{R}$ of hidden width $O\left(\epsilon^{-\frac{1}{k}} d^{1+\frac{1}{k}}\right)$ such that

$$|x^d - f(x, x^2, \dots, x^k)| < \epsilon$$

Lemma 3. (First order extension) For any $\epsilon > 0$ and a given natural number $d > k$, there exists a two-layer \mathbb{S}_n -equivariant linear MLP : $\mathbb{R}^{n \times k} \rightarrow \mathbb{R}^{n \times r}$ network with width $O\left(n^{\frac{1}{k}} \epsilon^{-\frac{1}{k}} r^{1+\frac{1}{k}}\right)$ such that

$$\left\| \text{MLP}\left(\mathbf{E}_k^{(1)}\right) - \mathbf{E}_r^{(1)} \right\| \leq \epsilon.$$

Proof. Assume that Λ^i is the diagonal matrix containing all eigenvalues of ψ_s^i . Applying Lemma 2, we simply see that Λ^q for $q = \overline{k+1, r}$ can be estimated using a two-layer MLP of width $O\left(\epsilon^{-\frac{1}{k}} r^{1+\frac{1}{k}}\right)$ with the max norm error less than ϵ . Formally, let $\widehat{\psi}_s^q$ be the estimation of ψ_s^q and e_i be the error at the i -th entry along the diagonal, then we have that

$$\left\| \widehat{\psi}_s^q - \psi_s^q \right\| = \left\| \sum_{i=1}^n e_i \mathbf{u}_i \mathbf{u}_i^\top \right\| \leq \sum_{i=1}^n |e_i| \|\mathbf{u}_i \mathbf{u}_i^\top\| \leq n\epsilon$$

Replacing ϵ with ϵ/n yields the desired result. \square

With enough first-order informations, i.e. sufficiently large r in Lemma 3, we can reconstruct the second-order features up to arbitrarily high degree.

Theorem 2. (First to second order) Assume that $\text{rank}(\psi_s - \mathbf{I}_n) \leq r$ and let $h : \mathbb{R}^{n \times r} \rightarrow \mathbb{R}^{n \times n \times r}$ be the resolution-wise outer product, then there exists a broadcasted linear feed forward layer $g : \mathbb{R}^r \rightarrow \mathbb{R}^d$ such that $(h \circ g)(\mathbf{E}_d^{(1)}) = \mathbf{E}_r^{(2)}$.

Proof. The first order features are aggregated through an outer product operator and return r square matrices of order n . However, these matrices are all rank one matrices and cannot represent the initial second order features. Since the rank of a square matrix is equivalent to its length minus the multiplicity of the eigenvalue zero, we can see that

$$\text{rank}(\psi_s - \mathbf{I}_n) = \text{rank}(\psi_s^2 - \mathbf{I}_n) = \dots = \text{rank}(\psi_s^d - \mathbf{I}_n) \leq r$$

Therefore, for all $i = \overline{1, d}$, the matrix $\psi_s^i - \mathbf{I}_n$ can be written as a weighted sum of r rank one matrices produced from the outer product. This concludes the proof. \square

A.2 Proof of Theorem 1

Theorem 3. For any $\epsilon > 0$ and real coefficients $\theta_0, \theta_1, \dots, \theta_d$ assume that $\text{rank}(\psi_s - \mathbf{I}_n) \leq r$, then there exists an \mathbb{S}_n -equivariant AE $f : \mathbb{R}^{n \times n \times k} \rightarrow \mathbb{R}^{n \times n \times r}$ of width $O(n^{1/k} r^{1+1/k} \epsilon^{-1/k})$ and a broadcasted feed forward network $g : \mathbb{R}^r \rightarrow \mathbb{R}$ such that

$$\|(g \circ f)(\mathbf{E}_k) - \mathbf{p}(\psi_s)\| < \epsilon$$

where $\mathbf{p}(\psi_s) = \sum_{j=0}^d \theta_j \psi_s^j$.

Proof. Encoder. The input tensor is of size $n \times n \times k$, representing second order feature in k different resolutions. The encoder simply operate resolution-wise and take the row-sum through each square matrix. This encoder will output a first order tensor of size $n \times k$. This layer is evidently \mathbb{S}_n -equivariant.

Latent. For the latent space, i.e. first-order feature space, we apply Lemma 3 to extend from k resolutions to r resolutions using a two-layer MLP of width $O\left(n^{\frac{1}{k}} \epsilon^{-\frac{1}{k}} r^{1+\frac{1}{k}}\right)$. And since this MLP is also built upon the broadcasting along the n -axis, it is also \mathbb{S}_n -equivariant.

Decoder. Applying the content of Theorem 2 we can conclude the proof. \square

Once the AE can learn to reconstruct, the following ensures that it can capture long-range information.

Theorem 4. For any $\epsilon > 0$ and real coefficients $\theta_1, \theta_2, \dots, \theta_d$, there exists a two-layer ReLU feed forward network $\varphi : \mathbb{R}^{n \times n \times d} \rightarrow \mathbb{R}^{n \times n}$ of hidden dimension $d_h = 2$ such that

$$\left\| \varphi(\mathbf{E}_d) - \sum_{j=1}^d \theta_j \mathbf{A}_j \right\| < \epsilon.$$

Proof. For this proof, we need to consider wavelet and random walk separately. **Wavelet.** Let $\psi_s = U\Lambda_s U^\top$ where $\Lambda_s = \text{diag}(\exp(-s\lambda_1), \exp(-s\lambda_2), \dots, \exp(-s\lambda_n))$. We first need to perform a transform on the vector basis $\mathbf{E}_d^{(2)}$. Essentially, the transformations are done independent of the eigenvectors U . Formally, we observe that

$$\begin{pmatrix} e^{-s\lambda_i} - 1 \\ e^{-2s\lambda_i} - 1 \\ \vdots \\ e^{-ds\lambda_i} - 1 \end{pmatrix} \approx \mathbf{A} \begin{pmatrix} \lambda_i - 1 \\ (\lambda_i - 1)^2 \\ \vdots \\ (\lambda_i - 1)^d \end{pmatrix} \quad (5)$$

where $\mathbf{A} \in \mathbb{R}^{d \times d}$ contains the corresponding Chebyshev polynomial expanding coefficients. Note that (5) is essentially the discrete fourier transform, thus the inversed version is simply

$$\begin{pmatrix} \lambda_i - 1 \\ (\lambda_i - 1)^2 \\ \vdots \\ (\lambda_i - 1)^d \end{pmatrix} \approx \mathbf{A}^{-1} \begin{pmatrix} e^{-s\lambda_i} - 1 \\ e^{-2s\lambda_i} - 1 \\ \vdots \\ e^{-ds\lambda_i} - 1 \end{pmatrix}. \quad (6)$$

This means that the power of \tilde{L} up to d can be retrieved via a broadcasted linear layer. Now let ζ be the scalar step function, meaning $\zeta(x) = 1$ for $x > 0$ and 0 otherwise. Then, let φ be a continuous piece-wise linear function such that:

$$\varphi(x) = \begin{cases} 0 & \text{if } x < 0 \\ x/\varepsilon & \text{if } 0 \leq x < 1 \\ 1 & \text{if } x \geq 1 \end{cases}$$

Since this function is a three-piece linear function, it can be represented as a ReLU-based feed forward network with hidden dimension two. And evidently,

$$\|\varphi - \zeta\| \rightarrow 0 \quad \text{as } \varepsilon \rightarrow 0.$$

Furthermore, it yields that $\zeta \left((\mathbf{I}_n - \tilde{L})^k \right) = \mathbf{A}_k$ for all k . Therefore, we concluded the proof. \square

B Additional implementation details

B.1 Datasets

Table 6 presents details of all benchmarking datasets used in our experiments. We focus on improving model performance in graph-level prediction tasks. All datasets contain over 1000 samples, with the average number of nodes per dataset ranging from 13 to over 100.

B.2 Hyperparameter Settings

Pretraining. 7 depicts the hyperparameters of our high-order autoencoder and training settings. In general, we used three layers of IGN [64] to build the encoder hidden dimensions of [8, 16, 32]. The decoder is a reversed of encoder with hidden dimensions [32, 16, 8]. We used a channel-wise 2-layer MLP to compute the latent \mathbf{Z} from the encoder’s output, and the latent dimension is set to 20. We preprocessed the Wavelet signals of graph data via the PyGSP [80] software. For each graph, we performed Wavelet transform to get its 4-resolution Wavelet tensor, where each scale varies in [0.25, 0.5, 0.75, 1]. Finally, the autoencoder is pretrained in 100 epochs with a batch size of 32 and learning rate of 0.0005.

MoleculeNet. 8 shows the hyperparameter settings for fine-tuning MPNN on five downstream datasets in MoleculeNet benchmark. In general, we used local attention as proposed in [81]. To model the global interactions, we augment virtual nodes to the local models to improve the performances in ToxCast and SIDER.

Dataset	# Graphs	# Nodes	# Edges	Pred. level	Pred. task	Metric
CIFAR10	60,000	117.63	469.10	graph	class. (10-way)	ACC
MNIST	70,000	70.57	281.65	graph	class. (10-way)	ACC
ZINC-subset	12,000	23.15	24.92	graph	reg.	MAE
MolBBBP	2,039	24.06	25.95	graph	class. (binary)	AUROC
MolBACE	1,513	34.09	36.86	graph	class. (binary)	AUROC
MolTox21	7,831	18.57	19.29	graph	class. (binary)	AUROC
MolToxCast	8,576	18.78	19.26	graph	class. (binary)	AUROC
MolSIDER	2,039	33.64	35.36	graph	class. (binary)	AUROC
Peptides-func	15,535	150.94	153.65	graph	class. (binary)	AP
Peptides-struct	15,535	150.94	153.65	graph	reg.	MAE
MUTAG	188	17.9	39.6	graph	class. (binary)	ACC
PROTEINS	1,113	39.1	72.8	graph	class. (binary)	ACC
NCI1	4,110	29.9	32.3	graph	class. (binary)	ACC
NCI109	4,127	29.7	32.1	graph	class. (binary)	ACC
IMDB-B	1,000	19.8	96.5	graph	class. (binary)	ACC
IMDB-M	1,500	13.0	65.9	graph	class. (3-way)	ACC

Table 6: Dataset details for transferability experiments on image, ZINC, MoleculeNet, LRGB and TUDataset.

Batch size	# Epoch	Encoder	Decoder	Learning rate	Scales	Latent dim	Masking Threshold
32	100	[8, 16, 32]	[32,16,8]	0.0005	[1,2,4,8]	20	100

Table 7: Hyperparameter settings for pretraining high-order AE.

TUDataset. Table 9 summarizes the hyperparameter settings for the transfer learning experiments on six TUDataset benchmark datasets. For IMDB-B and IMDB-M, which lack domain node features, we employed HOPE-WavePE as their initial node features. To create unified node features compatible with the hidden dimensions of the MPNN layers, we added a 2-layer MLP before the MPNN layers to update the combination of domain and HOPE-WavePE features. Following Bodnar et al. [75], we performed 10-fold validations for each dataset and reported means and standard deviations.

ZINC, Image Classification Tasks, and LRGB. We follow the best hyperparameter settings issued in previous work of GPS [34] and MPNN+VN [13]; then, we fine-tuned for better performance. Our full hyperparameter studies of the benchmarks are shown in Table 10.

Hyperparameter	BBBP	BACE	Tox21	ToxCast	SIDER
Pre MPNN	MLP	MLP	MLP	MLP	MLP
MPNN type	Attention	Attention	Attention	Attention	Attention
VN Augmented	-	-	-	✓	✓
# Layers	5	5	5	3	3
Hidden Dim	300	300	300	512	512
Dropout	0.5	0.5	0.5	0.5	0.5
Pooling type	mean	mean	mean	mean	mean
Learning rate	$1e-3$	$1e-3$	$1e-3$	$1e-3$	$1e-3$
Weight decay	$1e-9$	$1e-9$	$1e-9$	$1e-9$	$1e-9$
# Epochs	50	50	50	100	50
Batch size	32	32	32	32	32

Table 8: Hyperparameter settings for downstream evaluations on the MoleculeNet Benchmark.

Hyperparameter	MUTAG	PROTEINS	NC11	NC1109	IMDB-B	IMDB-M
Node Feat	Domain + PE	Domain + PE	Domain + PE	Domain + PE	PE	PE
Pre MPNN	MLP	MLP	MLP	MLP	MLP	MLP
# MPNN Layers	5	5	5	5	5	5
Hidden Dim	32	32	32	128	128	128
# Epochs	100	100	200	200	100	200
Batch size	128	128	128	128	128	128
Learning rate	$1e-3$	$1e-3$	$1e-3$	$1e-3$	$1e-3$	$1e-3$
Dropout	0.5	0.5	0.5	0.5	0.5	0.5
Graph pooling	mean	mean	mean	mean	mean	mean

Table 9: Hyperparameter settings for downstream evaluations on the TUDataset benchmark.

Hyperparameter	ZINC (subset)	MNIST	CIFAR10	Peptides-func	Peptides-struct
# Layers	9	3	3	3	3
Global Model	Transformer	Transformer	Transformer	Virtual Node	Virtual Node
Local Model	GINE	GatedGCN	GatedGCN	GINE	GINE
Hidden dim	64	50	50	128	128
# Heads	8	4	4	-	-
Dropout	0	0.2	0.2	0	0.01
Graph pooling	sum	mean	mean	mean	mean
PE dim	20	20	20	20	20
Node Update	MLP	MLP	MLP	MLP	MLP
Batch size	128	128	128	32	32
Learning Rate	0.0005	0.003	0.004	0.0005	0.0005
# Epochs	3000	300	300	100	100
# Warmup epochs	50	5	5	5	5
Weight decay	$3e-5$	$2e-4$	$3e-5$	$1e-5$	$1e-5$
# Parameters	452,299	150,081	142,093	477,953	432,206

Table 10: Hyperparameter settings for ZINC, MNIST, CIFAR10, Peptides-func and Peptides-struct dataset